ChemPubSoc Europe
DOI: 10.1002/chem.201900277
CHEMISTRY A European Journal Full Paper

Multicomponent Reactions |*Hot Paper*|

Sequential Cu-Catalyzed Four- and Five-Component Syntheses of Luminescent 3-Triazolylquinoxalines

Franziska K. Merkt,[a] Konstantin Pieper,[a] Maximilian Klopotowski,[b] Christoph Janiak,[b] and Thomas J. J. Müller*[a]

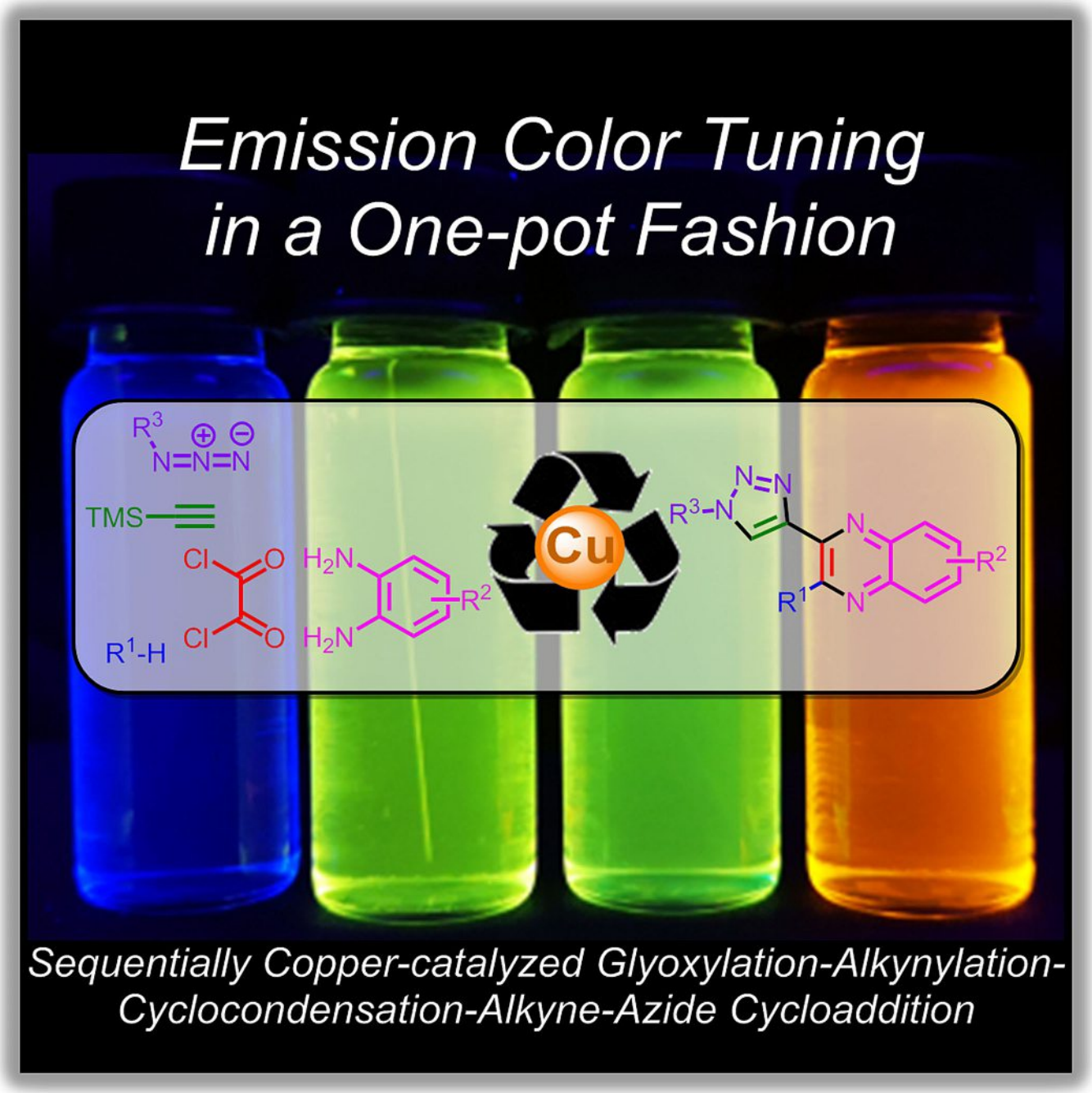

Abstract: 3-Triazolylquinoxalines can be readily synthesized by applying two complementary synthetic protocols starting from heterocyclic π nucleophiles or (hetero)aryl glyoxylic acids in a consecutive four- or five-component reaction. Conceptually, the sequential use of a single cuprous salt for alkynylation and Cu-catalyzed alkyne-azide cycloaddition (CuAAC) in a one-pot fashion sets the stage for activation-alkynylation-cyclocondensation-CuAAC or glyoxylation-alkynylation-cyclocondensation-CuAAC sequences in good yields. The diversity-oriented generation of differently substituted 3-triazolylquinoxalines is an excellent entry to tunable emission solvatorchromic fluorophores with triazole ligation. The electronic structure, corroborated by DFT and TD-DFT calculations, rationalizes the charge transfer character of relevant absorptions and large Stokes shifts as well as the electronic innocence of the triazole substituents.

Introduction

The advent of the Cu^{I}-catalyzed azide-alkyne cycloaddition (CuAAC) by Meldal[1] and Sharpless[2] has considerably popularized 1,4-disubstituted 1,2,3-triazoles as versatile building blocks in medicinal,[3] bioorganic[4] and materials chemistry.[5] The highly versatile and regioselective approach under mild conditions has enabled the formation of bioisosteres of the amide linker[3c,6] for application in bioconjugation. In addition, CuAAC are excellently suited to be employed in multicomponent reactions (MCRs).[7] Multicomponent syntheses of functional heterocyclic scaffolds also involve increasingly transition-metal catalysis.[8] In this respect, the economical reuse of a catalyst in the sense of sequential and tandem catalysis[9] is relevant for process development and the fundamental interest of reactivity tuning of a single catalyst source by sequential Pd-catalyzed reactions has also found entry in more complex one-pot syntheses of heterocycles.[10]

Quinoxalines have become increasingly important due to various intrinsic properties[11] and they can also be synthesized by MCR approaches.[12] In addition to the strongly electron-withdrawing nature of quinoxaline cores, the pyridyl nitrogen centers can be ideally addressed by pH change,[13] metal-ion coordination,[14] solvent-polarity changes,[12,13,15] or biological analytes.[16] Quinoxalines receive most interest as biologically active compounds[17] as well as functional chromophores.[18] The ligation of 1,2,3-triazoles and quinoxalines as electron-deficient moieties is particularly interesting and CuAAC[19] is a suitable methodology for introducing this moiety. However, the construction of 3-triazolylquinoxalines has only been reported in two publications with very few examples.[20,21]

Inspired by our chromogenic MCR concept[22] and our particular interest in highly emission solvatochromic quinoxalines,[12b,13,15,23] we reasoned that 3-triazolylquinoxalines could be accessible by combining the one-pot glyoxylation-alkynylation-cyclocondensation synthesis of 3-ethynylquinoxalines with CuAAC in a one-pot fashion (Figure 1).

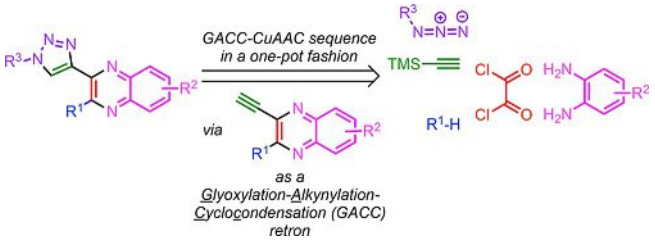

Figure 1. Retrosynthetic analysis of a one-pot synthesis of 3-triazolylquinoxalines in the sense of a consecutive five-component sequential Cu-catalyzed GACC-CuAAC (glyoxylation-alkynylation-cyclocondensation-CuAAC).

Glyoxylation of electron-rich π nucleophiles with oxalyl chloride followed by Castro alkynylation furnishes ynediones,[24] which are directly transformed by Hinsberg cyclization into 3-ethynylquinoxalines in the sense of a glyoxylation-alkynylation-cyclocondensation (GACC) sequence.[12b] The scope of ynedione intermediates can be considerably broadened by activation of glyoxylic acids with oxalyl chloride followed by Castro alkynylation,[25] which then concludes by Hinsberg cyclization following an activation-alkynylation-cyclocondensation (AACC) sequence.[15] In this regards, it is conceptually intriguing that both GACC and AACC syntheses of 3-ethynylquinoxalines are copper-catalyzed processes. Therefore, the concatenation of GACC or AACC with CuAAC should lead to a sequential Cu-catalyzed process.[9] Here, we report the first GACC-CuACC and AACC-CuAAC syntheses of 3-(1,2,3-triazolyl)quinoxalines, their photophysical properties and their TD-DFT-calculated electronic structure.

Results and Discussion

Synthesis and structure

We first set out to test the initial conditions of CuAAC with 3-ethynylquinoxaline **1**[13] and benzyl azide (**2a**) (Figure 2). Indeed, compounds **1** and **2a** are almost quantitatively trans-

[a] Dr. F. K. Merkt, K. Pieper, Prof. Dr. T. J. J. Müller
Institut für Organische Chemie und Makromolekulare Chemie
Heinrich-Heine-Universität Düsseldorf
Universitätsstraße 1, 40225 Düsseldorf (Germany)
E-mail: ThomasJJ.Mueller@uni-duesseldorf.de

[b] M. Klopotowski, Prof. Dr. C. Janiak
Institut für Anorganische Chemie und Strukturchemie
Heinrich-Heine-Universität Düsseldorf
Universitätsstraße 1, 40225 Düsseldorf (Germany)

Supporting information and the ORCID identification number(s) for the author(s) of this article can be found under:
https://doi.org/10.1002/chem.201900277.

Part of a Special Issue in honor of the 20th IUPAC International Symposium on Organometallic Chemistry directed towards Organic Synthesis (OMCOS 20). To view the complete issue, visit Issue 40.

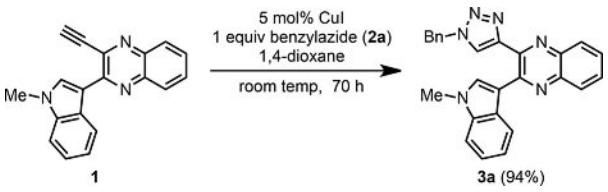

Figure 2. CuAAC of 3-ethynylquinoxaline **1** and benzyl azide (**2a**) to give 3-(1,2,3-triazolyl)quinoxaline derivative **3a**.

formed at room temperature in 1,4-dioxane in the presence of 5 mol% of CuI, the same catalyst source and loading as in the GACC and AACC sequences, to give the 3-(1,2,3-triazolyl)quinoxaline derivative **3a** in 94% yield. With these conditions for the CuAAC step in hand, we started to optimize the GACC-CuAAC sequence employing *N*-methylindole (**4a**), oxalyl chloride (**5**), (trimethylsilyl)acetylene (**6**), *o*-phenylenediamine (**7a**) and benzyl azide (**2a**) to give 2-(1-benzyl-1*H*-1,2,3-triazol-4-yl)-3-(1-methyl-1*H*-indol-3-yl)quinoxaline (**3a**) in a model reaction (see Supporting Information, Table S1). It was found that a suitable amount of potassium fluoride for desilylation with a slight excess of the benzyl azide (**2a**) in a THF/MeOH mixture turned out to be optimal. Using a small amount of sodium ascorbate (10 mol%) for the CuAAC step finally resulted in a clean transformation. With these optimized conditions and starting from π nucleophiles **4**, the consecutive sequential Cu-catalyzed five-component GACC-CuAAC synthesis was demonstrated for 18 preparative examples, furnishing the title compounds **3** in moderate to excellent yields (Table 1).

As π nucleophiles, *N*-methylindole (**4a**), *N*-methyl- (**4b**) or phenylpyrrole (**4c**) as well as 2-methoxythiophene (**4d**) were employed easily (Table 1, entries 1–4). Much to our delight, also indolizine (**4e**), an isomer of indole led to the formation of the corresponding 3-triazolylquinoxaline **3e** in 42%. The modular nature of the reaction allowed for the introduction of a variety of azides. Among electron-rich to electron-poor benzylic substituents, aromatic azides could also be employed. Moreover, sterically hindered, aliphatic, as well as secondary substituted azides were used to construct 3-triazolylquinoxalines **3**. Ester- (**2j**) and amide-functionalized azides (**2k**) were also compatible with the reaction sequence and produced compounds **3o** and **3p** in 53 and 38% yields, respectively. This demonstrates the conceivable use of this sequence for bioconjugation of peptides to suitable quinoxaline fluorophores. 1,2-Diaminobenzene (**7a**) and 2,3-diaminonaphthalene (**7b**) were also employed in the synthesis of 3-triazolylquinoxalines. Other 1,2-diaminoarenes, such as 4,5-dichlorobenzene-1,2-diamine and 4,5-diaminophthalonitrile that have been successfully applied in the formation of 3-ethynylquinoxalines[12b] or 3-aminovinylquinoxalines[13] could not be transformed in this sequence. In comparison to the four-step 3-ethynylquinoxaline synthesis,[12b,15a] the higher yields of the five-step 3-triazolylquinoxaline formation also account for the increased stability of the title compounds.

Although the GACC sequence for the formation of 3-ethynyl quinoxalines is limited to certain electron-rich π nucleophiles, the AACC sequence starting from 2-(hetero)aryl glyoxylic acid is a valuable complementary access to other electronic substitution patterns in 2-position of quinoxalines.[15] Therefore, the AACC-CuAAC sequence was illustrated for three examples (Figure 3). Starting from glyoxylic acids **8**, activation with oxalyl chloride (**5**) and subsequent Castro alkynylation of the glyoxalyl chloride with (trimethylsilyl)acetylene (**6**), followed by Hinsberg cyclization with *o*-phenylenediamine (**7a**) and CuAAC with benzyl azide (**2a**) furnished the corresponding 3-(1,2,3-triazolyl)quinoxalines **3s**–**u** in good yields.

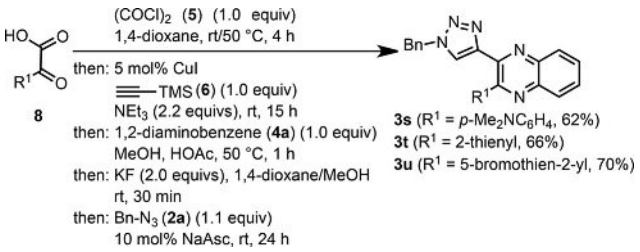

Figure 3. Consecutive four-component AACC-CuAAC synthesis of 3-(1,2,3-triazolyl)quinoxalines **3**.

Most advantageously, both sequences allow the use of the components in almost equimolar amounts. The average yields per bond-forming step were calculated for the GACC-CuAAC sequence to be 85–97%, whereas the AACC-CuAAC sequence gave 90–93%. Therefore, both one-pot multicomponent syntheses can be considered as highly efficient.

The structures of all 3-triazolylquinoxalines **3** were unequivocally characterized by ^{1}H and ^{13}C NMR spectroscopy, mass spectrometry, and combustion analysis. It is noteworthy that the purification processes involved only silica-gel column chromatography in air, verifying that these 3-triazolylquinoxalines are substantially stable towards air and moisture. Interestingly, the single-crystal X-ray diffraction of *N*-methylpyrrole substituted 3-triazolylquinoxaline **3b** provides insight into the molecular structure in the solid state (Figure 4 and Figure 5). As expected, the quinoxaline moiety is planar with a slight thermic oscillation at the benzo-backbone, while the *N*-methylpyrrole substituent (66°) and the triazolyl moiety are twisted out of coplanarity.

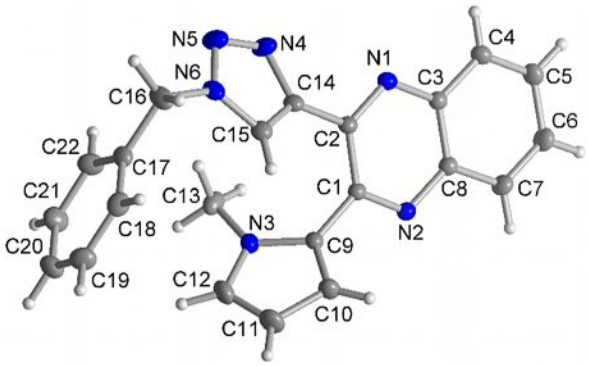

Figure 4. Molecular structure of compound **3b** (thermal ellipsoids for N and C shown at 50% probability). See the Supporting Information for further details on the crystal structure.

Table 1. Consecutive five-component GACC-CuAAC synthesis of 3-(1,2,3-triazolyl)quinoxalines **3**.

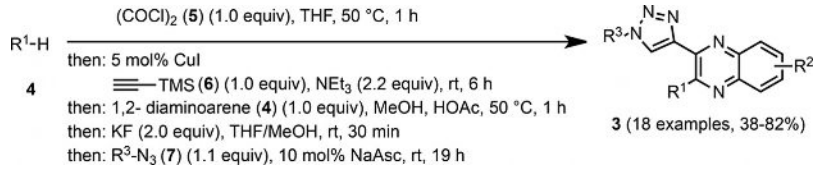

Entry	π Nucleophile **4**	1,2-Diaminoarene **7**	Azide **2**	3-(1,2,3-Triazolyl)quinoxaline **3** (Yield)
1	*N*-methylindole (**4a**)	*ortho*-phenylenediamine (**7a**)	benzyl azide (**2a**)	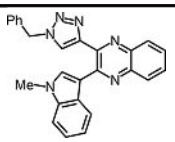 **3a** (82%)
2	*N*-methylpyrrole (**4b**)	**7a**	**2a**	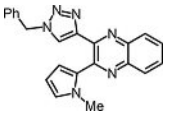 **3b** (77%)
3	*N*-phenylpyrrole (**4c**)	**7a**	**2a**	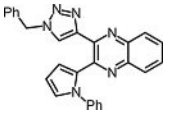 **3c** (56%)
4	2-methoxythiophene (**4d**)	**7a**	**2a**	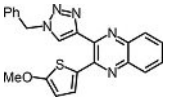 **3d** (72%)
5	indolizine (**4e**)	**7a**	**2a**	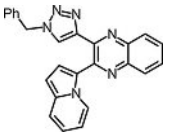 **3e** (42%)
6	**4a**	**7a**	(2-azidoethyl)benzene (**2b**)	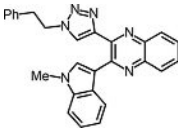 **3f** (73%)
7	**4a**	**7a**	1-(azidomethyl)-4-chlorobenzene (**2c**)	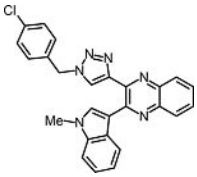 **3g** (48%)
8	**4a**	**7a**	1-(azidomethyl)-2-methylbenzene (**2d**)	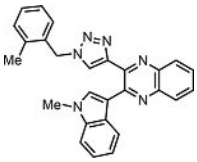 **3h** (79%)
9	**4a**	**7a**	1-(azidomethyl)-3-fluorobenzene (**2e**)	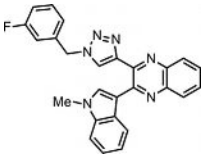 **3i** (58%)
10	**4a**	**7a**	1-azido-4-methoxybenzene (**2f**)	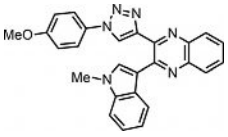 **3j** (46%)
12	**4a**	**7a**	(1-azidoethyl) benzene (**2h**)	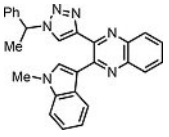 **3k** (69%)

Table 1. (Continued)

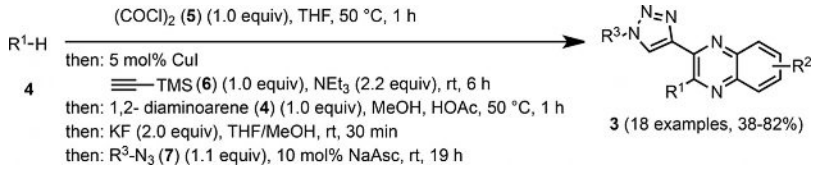

Entry	π Nucleophile **4**	1,2-Diaminoarene **7**	Azide **2**	3-(1,2,3-Triazolyl)quinoxaline **3** (Yield)
11	**4a**	**7a**	(azidomethylene) dibenzene (**2g**)	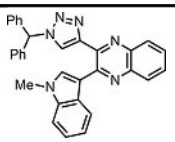 **3l** (56%)
13	**4a**	**7a**	1-azidohexane (**2i**)	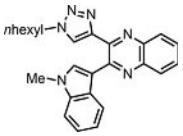 **3m** (81%)
14	**4b**	**7a**	**2i**	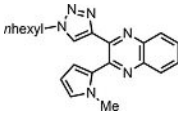 **3n** (80%)
15	**4a**	**7a**	methyl 2-azidoacetate (**2j**)	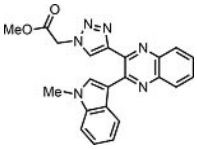 **3o** (53%)
16	**4b**	**7a**	2-azido-*N,N*-dimethylacetamide (**2k**)	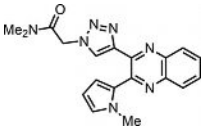 **3p** (38%)
17	**4a**	2,3-diamino naphthalene (**7b**)	**2a**	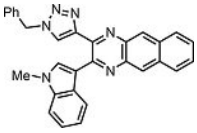 **3q** (74%)
18	**4b**	**7b**	**2a**	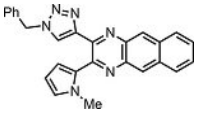 **3r** (74%)

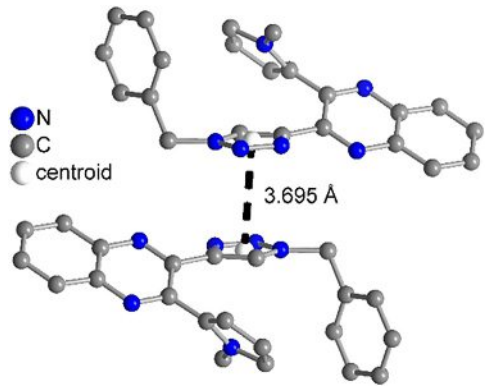

Figure 5. Centrosymmetric pairwise π–π stacking in the structure of compound **3b**.

There are three different ring–ring torsion angles between the *N*-methylpyrrole (N), the quinoxaline (Q), the benzyl (B) and the triazolyl (T) rings. The angle between Q and B is the highest with 117° determined from the atoms C17-C16-N6-N5. Between Q and N, the angle is 60° (C2-C1-C9-N3) and between Q and T (C1-C2-C14-C14), an angle of 33° is found. A closer analysis of the crystallographic packing revealed a centrosymmetric pairwise arrangement by strong π–π interactions between the triazolyl rings (Figure 5).

The two parallel triazolyl rings assume a close contact with a centroid distance of 3.695 Å, an interplanar separation of 3.615 Å, small slip angle of 11.9° (between centroid-centroid vector and plane normal) and a small slippage of 0.76 Å, which translate into a sizable overlap of the triazolyl-plane areas and can be classified as strong π stacking.[26] No other π–π stacking exists in the structure.

Photophysical properties

Previous studies on related quinoxaline chromophores have shown interesting photophysical properties especially for donor-acceptor-substituted derivatives,[12b,13,15] which display bathochromically shifted emission maxima and large Stokes shifts. Therefore, the polar anti-auxochromic substituent effect of triazolyl units could be interesting with respect to its solvatochromic effect. The photophysical properties of two consanguineous series of 3-triazolylquinoxalines **3** recorded in CH_2Cl_2 were studied by absorption and fluorescence spectroscopy (Figures 6–8). In series 1, the triazole substituent R^3 in position

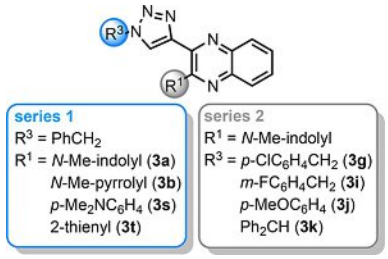

Figure 6. Two consanguineous series of 3-triazolylquinoxalines **3**.

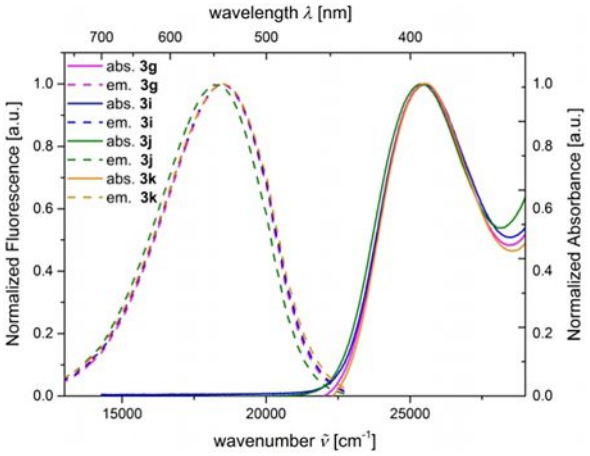

Figure 7. Normalized UV/Vis absorption (solid lines), $c(\mathbf{3}) = 10^{-5}$ M, and emission (dashed lines), $c(\mathbf{3}) = 10^{-7}$ M, $\lambda_{exc} = 420$ nm, spectra of 3-triazolylquinoxalines **3g**, **3i**–**3k**. Recorded in dichloromethane, $T = 298$ K.

3 of the quinoxaline core was chosen as benzyl and the quinoxaline substituent R^1 was altered, whereas in series 2 the substituent R^1 in position of 2 of the quinoxaline core was kept constant as *N*-methylindol-3-yl and the triazole substituent R^3 was varied. The relative fluorescence quantum yields Φ_f were determined with suitable standards according to literature procedures.[27]

All eight investigated 3-triazolylquinoxalines **3** possess their longest wavelength absorption maximum between $\lambda = 368$ and 400 nm with molar absorption coefficients ε ranging from 6800 to 12000 $L\,mol^{-1}\cdot cm$ and at least one additional absorption band at higher energy can be detected (Table 2). Series 1 and 2 were used to underline the electronic effects of substitu-

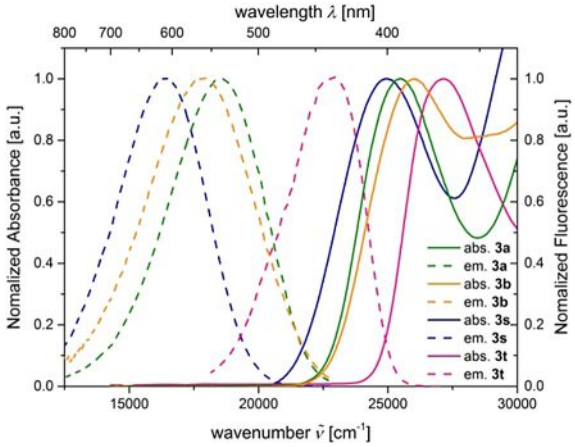

Figure 8. Normalized UV/Vis absorption (solid lines), $c(\mathbf{3}) = 10^{-5}$ M, and emission (dashed lines), $c(\mathbf{3}) = 10^{-7}$ M, $\lambda_{exc} = 420$ nm, spectra of 3-triazolylquinoxalines **3a**–**3b** and **3s**–**3t**. Recorded in dichloromethane, $T = 298$ K.

ents R^1 and R^3. The spectral comparison reveals that the triazolyl substituent R^3 has almost no effect on the absorption and emission energies (Figure 7), whereas the quinoxalinyl substituent R^1 significantly affects both absorption and emission bands (Figure 8). By increasing the electron-donating character of the heterocyclic substituent R^1, the absorption and the emission bands shift bathochromically from 2-thienyl (**3t**, $\lambda_{max,abs} =$ 368 nm, $\lambda_{max,em} = 541$ nm) over 1-methylpyrrolyl (**3b**, $\lambda_{max,abs} =$ 384 nm, $\lambda_{max,em} = 548$ nm) to 1-methylindolyl (**3a**, $\lambda_{max,abs} =$ 393 nm, $\lambda_{max,em} = 541$ nm) and *p*-$Me_2NC_6H_4$ (**3s**, $\lambda_{max,abs} =$ 393 nm, $\lambda_{max,em} = 541$ nm, Figure 8). The Stokes shifts vary in a range from 7000 to 8700 cm^{-1}, except for the 2-thienyl derivative **3t**, which is significantly smaller with 4500 cm^{-1}. The fluorescence quantum yields Φ_f of the 3-triazolylquinoxalines are relatively small compared to 3-aminovinyl derivatives[23] or 3-ethynylquinoxalines.[12b,15] The highest value can be found for the *p*-$Me_2NC_6H_4$ derivative **3s** (Table 2). Presumably, the low values of fluorescence quantum yields Φ_f result from the torsion by the triazolyl substituent, which hampers the planarization of the π-system in the ground and excited states.

Electronic structure of 3-triazolylquinoxalines 3

A deeper understanding of the photophysical behavior of selected 3-triazolylquinoxalines **3a**,**b** and **3s** was sought by elucidating the electronic structure by calculating UV/Vis absorption spectra on the DFT level of theory, with a special focus on comparison to the respective donor moiety R^1 and on the origin of the longest wavelength absorption maxima of each structure. The geometries of the electronic ground-state structures were optimized using Gaussian09[29] with PBEh1PBE[30] as functional and the Pople 6–311G++G(d,p) basis set.[31] Given that absorption properties were measured in dichloromethane solutions, the polarizable continuum model (PCM) with dichloromethane as a solvent was applied.[32] All minimum structures were unambiguously assigned by analytical frequency analysis. The structures were chosen as a series of compounds with two different heterocyclic substituents and a *p*-$Me_2NC_6H_4$

Table 2. UV/Vis absorption and emission data of selected 2-substituted 3-triazolylquinoxalines **3**.

	$\lambda_{max,abs}$[a] [nm] (ε [L mol^{-1} cm^{-1}])	$\lambda_{max,em}$[b] [nm] (Φ_f)[c]	Stokes shift $\Delta\tilde{\nu}$[d] [cm^{-1}]
3a	262 (21 700) 292 (15 300) 393 (10 100)	541 (< 0.01)	7000
3b	259 (23 000) 293 (9400sh) 384 (6800)	548 (< 0.01)	8300
3s	260 (22 400sh) 309 (16 600) 400 (8600)	613 (0.02)	8700
3t	273 (18 400) 293 (14 800sh) 368 (12 000)	440 (< 0.01)	4500
3g	265 (32 000) 396 (10 200)	541 (< 0.01)	7000
3i	265 (32 000) 396 (10 200)	547 (< 0.01)	7000
3j	263 (22 600) 290 (14 600) 392 (9200)	541 (< 0.01)	7000
3k	264 (21 400) 292 (15 200) 391 (10 000)	540 (< 0.01)	7000

[a] Recorded in CH_2Cl_2, $c(\mathbf{3}) = 10^{-5}$ M at $T = 293$ K. [b] Recorded in CH_2Cl_2, $c(\mathbf{3}) = 10^{-7}$ M at $T = 293$ K. [c] Relative fluorescence quantum yields were determined employing literature procedures (±10%)[27] with coumarin 153 as a standard in methanol, $\lambda_{exc} = 420$ nm ($\Phi_f = 0.45$),[28] $\Delta\tilde{\nu} = 1/\lambda_{max,abs} - 1/\lambda_{max,em}$.

substituent in 2-position of the quinoxaline core. The R^3 substituent on the triazole moiety was kept constant as a benzyl substituent. The computed equilibrium ground state structure of **3b** matches very well with the structure obtained from X-ray analyses. The experimentally determined torsional angle between the *N*-methylpyrrole substituent and quinoxaline core is well reproduced by the computations ($\Theta_{calc} = 66^\circ$ vs. $\Theta_{X\text{-}ray} = 60^\circ$). A closer inspection of the coefficient densities in the Kohn–Sham frontier molecular orbitals of the three 3-triazolylquinoxalines **3a**,**b** and **3s** reveals that the HOMO coefficient densities are predominantly localized on the heterocyclic substituent R^1 (Figure 9). Accordingly, the coefficient densities in the LUMOs are localized on the quinoxaline acceptor cores. In any case, the 3-triazole moiety only possesses a minor coefficient density. Expectedly, a major electronic effect of the triazole on the relevant electronic absorption and emission bands is not very likely. This feature, however, is favorable for employing triazole ligation between the chromophore and the substrate because the former will be undisturbed. The predominant localization of the coefficient densities in HOMO and LUMO already indicates proposed potential charge transfer (CT) character of the relevant absorption bands.

The optimized structures of **3a**, **3b** and **3s** were submitted to TD-DFT calculations to study the absorption characteristics in more detail again applying PCM with dichloromethane as a solvent (Table 3).

The computed results satisfactorily match with the experimental absorption maxima. As expected, the longest wavelength absorption bands of all three calculated 3-triazolylquinoxalines originate from dominant contributions of HOMO–LUMO based transitions. The relevant oscillator strengths additionally indicate permitted electronic transitions. In comparison, related 3-ethynylquinoxaline chromophores adopt significantly higher values of the oscillator strengths[12b,15] due to less steric strain of the alkynyl substituent in comparison to the triazolyl moiety. In all three calculated cases, two additional absorption maxima at lower wavelengths emanate predominantly from HOMO→LUMO+1, HOMO-1→LUMO, HOMO→LUMO+2, and HOMO-1→LUMO+1 transitions.

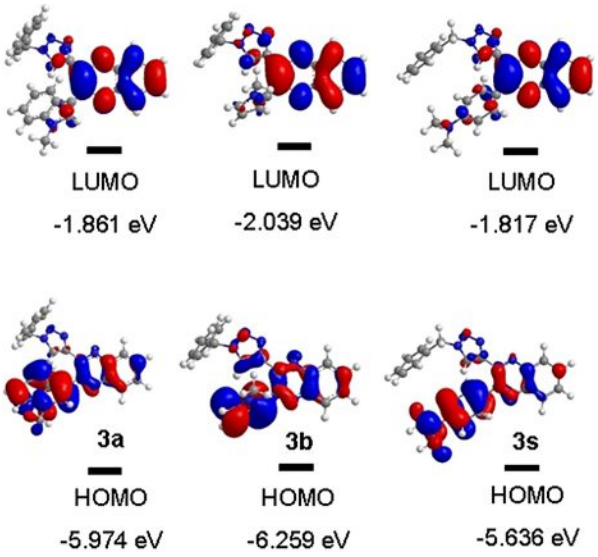

Figure 9. Selected DFT-computed (PBEh1PBE/6–311++G(d,p)) Kohn–Sham frontier molecular orbitals of 3-triazolylquinoxalines **3a**,**b** and **3s**.

Conclusion

We have developed a straightforward approach to synthesize of 3-triazolylquinoxalines based upon a sequential Cu-cata-

Table 3. TD-DFT calculations [PBEh1PBE/6–311++G(d,p)] of the absorption maxima of 3-triazolylquinoxalines **3a**,**b** and **3s** by applying PCM with dichloromethane as solvent.

	$\lambda_{max,abs}$[a] [nm] (ε [L mol^{-1} cm^{-1}])	$\lambda_{max,calcd}$ [nm]	Most dominant contributions	Oscillator strength
3a	262 (21 700)	288	HOMO→LUMO+1 (70%)	0.259
	292 (15 300)	309	HOMO-1→LUMO (77%)	0.069
	393 (10 100)	370	HOMO→LUMO (95%)	0.143
3b	259 (23 000)	250	HOMO-1→LUMO+1 (37%)	0.339
	293 (9400sh)	288	HOMO→LUMO+1 (79%)	0.097
	384 (6800)	371	HOMO→LUMO (85%)	0.074
3s	260 (22 400sh)	296	HOMO→LUMO+2 (63%)	0.162
	309 (16 600)	311	HOMO→LUMO+1 (82%)	0.128
	400 (8600)	391	HOMO→LUMO (98%)	0.184

[a] Recorded in CH_2Cl_2, $c(\mathbf{3}) = 10^{-5}$ M at $T = 293$ K.

lyzed process, consisting of Cu-catalyzed alkynylation and CuAAC proceeding in a one-pot fashion. Particularly interesting is that either electron-rich π nucleophiles by applying the glyoxylation-alkynylation-cyclocondensation-CuAAC sequence or glyoxylic acids through the activation-alkynylation-cyclocondensation-CuAAC sequence can be complementarily employed to prepare extended substance libraries. Moreover, 3-triazolylquinoxalines possess interesting photophysical properties. All generated triazolyl-based products are luminescent in solution and their photophysical characteristic were assessed in dichloromethane solution. The corresponding absorption and emission maxima can be fine-tuned in accordance with the substituent in the 2-position of the quinoxaline core. Interestingly, the triazolyl moiety does not affect the absorption or emission maxima, and hence qualifies as an excellent mostly electronic-innocent linker for various biological substrates, polymers and surfaces. The electronic structure, assessed by DFT and TD-DFT calculations, rationalizes the pronounced emission solvatochromicity and large Stokes shift as a consequence of CT character of the relevant longest wavelength absorption bands. The highly diversity-oriented nature of the synthetic process and the one-pot characteristics of the sequentially Cu-catalyzed multicomponent synthesis opens new avenues for applications of tailored emissive chromophore libraries in biophysical analytics. Further studies are currently under investigation.

Experimental Section

Experimental details and full characterization of compounds **1** and **3**, ^{1}H and ^{13}C NMR spectra of compounds **1** and **3**, selected UV/Vis and emission spectra of compounds **3**, X-ray structure data tables of compound **3b**, DFT computed XYZ-coordinates, energies, and absorption spectra of structures of selected compounds **3** can be found in the Supporting Information.

Typical procedure for the five-component synthesis of 2-(1-benzyl-1*H*-1,2,3-triazol-4-yl)-3-(1-methyl-1*H*-indol-3-yl)quinoxaline (3a): 2.00 mmol of *N*-methylindole (4a) (268 mg, 1.00 equiv) in dry THF (5.00 mL mmol^{-1}) was placed under nitrogen atmosphere in a sintered screw-cap Schlenk tube, degassed with nitrogen, and cooled to 0 °C (water/ice, 5 min). Then, oxalyl chloride (5) (0.18 mL, 2.00 mmol, 1.00 equiv) was added dropwise to the reaction mixture at 0 °C. The mixture was then stirred for 1 h at 50 °C (oil bath). Thereafter, the mixture was cooled to room temperature (water bath, 5 min). Then, CuI (20 mg, 0.10 mmol, 5 mol%), one equivalent of TMSA (6), and dry triethylamine (0.60 mL, 4.40 mmol, 2.20 equiv) were successively added to the reaction mixture, and stirring at room temperature was continued for 6 h. Then, 2 mL of methanol, 2.00 mmol of the *o*-diaminoarene (7a) (216 mg, 1.00 equiv), and acetic acid (0.24 mL, 4.00 mmol, 2.00 equiv) were added successively and the mixture was stirred at 50 °C for 1 h. Potassium fluoride (236 mg, 4.00 mmol, 2.00 equiv) was added with 1.0 mL THF and 2 mL methanol. The reaction mixture was stirred for 30 min at room temperature. Lastly, benzylazide (**2a**; 292 mg, 2.20 mmol, 1.10 equiv; for experimental details, see Table S2 in the Supporting Information) was added with 6 mL of THF and NaAsc (40 mg, 0.20 mmol, 10 mol%; Asc = ascorbate) and the reaction mixture was stirred at room temperature for another 19 h. Then 10 mL water was added, the phases were separated, and the aqueous phase was extracted with dichloromethane (3×10 mL, monitored by TLC). The combined organic layers were dried with anhydrous sodium sulfate. After removal of the solvents in vacuo, the residue was absorbed onto Celite and purified chromatographically on silica gel with petroleum ether (boiling range 40–60 °C)/ethyl acetate to give the 3-triazolylquinoxaline **3a** (680 mg, 83%) as a yellow solid, M.p.: 175 °C; ^{1}H NMR ($CDCl_3$, 300 MHz): $\delta = 3.67$ (s, 3H), 5.42 (s, 2H), 7.01–7.11 (m, 3H), 7.16–7.23 (m, 1H), 7.24–7.30 (m, 5H), 7.42 (s, 1H), 7.62–7.77 (m, 3H), 8.05–8.16 ppm (m, 2H); ^{13}C NMR ($CDCl_3$, 75 MHz): $\delta = 33.1$ (CH_3), 54.1 (CH_2), 109.6 (CH), 113.2 (C_{quat}), 120.9 (CH), 121.3 (CH), 122.5 (CH), 124.4 (CH), 126.7 (C_{quat}), 127.9 (CH), 128.7 (CH), 129.1 (CH), 129.2 (CH), 129.3 (CH), 130.3 (CH), 131.3 (CH), 134.3 (C_{quat}), 137.1 (C_{quat}), 140.1 (C_{quat}), 141.6 (C_{quat}), 144.6 (C_{quat}), 146.6 (C_{quat}), 149.1 ppm (C_{quat}); EI+MS [*m/z* (%)]: 417 ([*M*+H]$^+$, 26), 416 ([M]$^+$, 100), 387 ([$C_{26}H_{20}N_4$]$^+$, 15), 373 ([$C_{26}H_{20}N_3$]$^+$, 11), 298 (20), 297 ([$C_{19}H_{13}N_4$]$^+$, 93), 296 (18), 295 (10), 287 (21), 285 (13), 284 ([$C_{17}H_{11}N_5$]$^+$, 49), 283 (34), 282 (38), 281 (14), 271 (46), 270 ([$C_{17}H_{11}N_4$]$^+$, 95), 269 (32), 268 ([$C_{18}H_{10}N_3$]$^+$, 15), 259 ([$C_{17}H_{12}N_3$]$^+$, 29), 256 ([$C_{17}H_{11}N_3$]$^+$, 22), 255 (11), 155 ([$C_9H_7N_3$]$^+$, 12), 91 ([C_7H_7]$^+$, 34); IR (ATR): $\tilde{\nu} = 3134$ (w), 3061 (w), 3044 (w), 2955 (w), 2928 (w), 2913 (w), 2901 (w), 2884 (w), 1526 (m), 1497 (w), 1476 (m), 1456 (m), 1447 (m), 1423 (m), 1408 (w), 1368 (m), 1337 (m), 1296 (w), 1275 (w), 1240 (m), 1211 (m), 1188 (w), 1161 (w), 1128 (m), 1092 (m), 1067 (m), 1043 (m), 1016 (w), 978 (m), 935 (m), 880 (w), 814 (w), 773 (m), 731 (s), 708 (s), 692 (m), 669 (m), 623 cm^{-1} (m); Anal. calcd for $C_{26}H_{20}N_6$ (416.5): C 74.98, H 4.84, N 20.18. Found: 74.70, H 5.13, N 19.92.

Acknowledgements

We cordially thank the Fonds der Chemischen Industrie and the Deutsche Forschungsgemeinschaft (Mu 1088/9-1) for financial support.

Conflict of interest

The authors declare no conflict of interest.

Keywords: alkynylation · click reaction · copper · fluorescence · sequential catalysis

[1] C. W. Tornøe, C. Christensen, M. Meldal, *J. Org. Chem.* **2002**, *67*, 3057–3062.

[2] H. C. Kolb, M. G. Finn, K. B. Sharpless, *Angew. Chem. Int. Ed.* **2001**, *40*, 2004–2021; *Angew. Chem.* **2001**, *113*, 2056–2075.

[3] For recent reviews on the medicinal applications of click chemistry, see: a) H. C. Kolb, K. B. Sharpless, *Drug. Discovery Today* **2003**, *8*, 1128–1137; b) P. Thirumurugan, D. Matosiuk, K. Jozwiak, *Chem. Rev.* **2013**, *113*, 4905–4979; c) G. C. Tron, T. Pirali, R. A. Billington, P. L. Canonico, G. Sorba, A. A. Genazzani, *Med. Res. Rev.* **2008**, *28*, 278–308.

[4] a) J. E. Moses, A. D. Moorhouse, *Chem. Soc. Rev.* **2007**, *36*, 1249–1262; b) J. D. White, M. F. Osborn, A. D. Moghaddam, L. E. Guzman, M. M. Haley, V. J. De Rose, *J. Am. Chem. Soc.* **2013**, *135*, 11680–11683; c) C. Besanceney-Webler, H. Jiang, T. Zheng, L. Feng, D. Soriano del Amo, W. Wang, L. M. Klivansky, F. L. Marlow, Y. Liu, P. Wu, *Angew. Chem. Int. Ed.* **2011**, *50*, 8051–8056; *Angew. Chem.* **2011**, *123*, 8201–8206.

[5] a) B. O. Okesola, A. Mata, *Chem. Soc. Rev.* **2018**, *47*, 3721–3736; b) P. Wu, A. K. Feldman, A. K. Nugent, C. J. Hawker, A. Scheel, B. Voit, J. Pyun, J. M. J. Frechet, K. B. Sharpless, V. V. Fokin, *Angew. Chem. Int. Ed.* **2004**, *43*, 3928–3932; *Angew. Chem.* **2004**, *116*, 4018–4022; c) B. Helms, J. L. Mynar, C. J. Hawker, J. M. J. Fréchet, *J. Am. Chem. Soc.* **2004**, *126*,

15020 – 15021; d) P. Wu, M. Malkoch, J. N. Hunt, R. Vestberg, E. Kaltgrad, M. G. Finn, V. V. Fokin, K. B. Sharpless, C. J. Hawker, *Chem. Commun.* **2005**, 5775 – 5777; e) D. I. Rozkiewicz, D. Janczewski, W. Verboom, B. J. Ravoo, D. N. Reinhoudt, *Angew. Chem. Int. Ed.* **2006**, *45*, 5292 – 5296; *Angew. Chem.* **2006**, *118*, 5418 – 5422.

[6] a) W. S. Horne, M. K. Yadav, C. D. Stout, M. R. Ghadiri, *J. Am. Chem. Soc.* **2004**, *126*, 15366 – 15367; b) C. W. Tornøe, S. J. Sanderson, J. C. Mottram, G. H. Coombs, M. Meldal, *J. Comb. Chem.* **2004**, *6*, 312 – 324.

[7] S. Hassan, T. J. J. Müller, *Adv. Synth. Catal.* **2015**, *357*, 617 – 666.

[8] D. M. D'Souza, T. J. J. Müller, *Chem. Soc. Rev.* **2007**, *36*, 1095 – 1108.

[9] For reviews on tandem and sequential catalysis, see: a) J.-C. Wasilke, S. J. Obrey, R. T. Baker, G. C. Bazan, *Chem. Rev.* **2005**, *105*, 1001 – 1020; b) A. Ajamian, J. L. Gleason, *Angew. Chem. Int. Ed.* **2004**, *43*, 3754 – 3760; *Angew. Chem.* **2004**, *116*, 3842 – 3848; c) D. E. Fogg, E. N. de Santos, *Coord. Chem. Rev.* **2004**, *248*, 2365 – 2379; d) T. J. J. Müller, *Top. Organomet. Chem.* **2006**, *19*, 149 – 205; e) T. J. J. Müller, in *Molecular Catalysts: Structure and Functional Design*, L. H. Gade, P. Hofmann, Hrsg., Wiley-VCH Verlag GmbH & Co. KGaA, Weinheim, **2014**, 255 – 279.

[10] a) T. Lessing, T. J. J. Müller, *Appl. Sci.* **2015**, *5*, 1803 – 1836; for recent examples on alkynylation-cyclization-CuAAC sequences, see: b) P. Niesobski, F. Klukas, H. Berens, G. Makhloufi, C. Janiak, T. J. J. Müller, *J. Org. Chem.* **2018**, *83*, 4851 – 4858; c) T. Lessing, H. van Mark, T. J. J. Müller, *Chem. Eur. J.* **2018**, *24*, 8974 – 8979.

[11] K. R. Justin Thomas, M. Velusamy, J. T. Lin, C.-H. Chuen, Y.-T. Tao, *Chem. Mater.* **2005**, *17*, 1860 – 1866.

[12] a) R. S. Bhosale, S. R. Sarda, S. S. Ardhapure, W. N. Jadhav, S. R. Bhusare, R. P. Pawar, *Tetrahedron Lett.* **2005**, *46*, 7183 – 7186; b) C. F. Gers, J. Nordmann, C. Kumru, W. Frank, T. J. J. Müller, *J. Org. Chem.* **2014**, *79*, 3296 – 3310; c) K. Saravana Mani, W. Kaminsky, S. P. Rajendran, *New J. Chem.* **2018**, *42*, 301 – 310.

[13] C. F. Gers-Panther, H. Fischer, J. Nordmann, T. Seiler, T. Behnke, C. Werth, W. Frank, U. Resch-Genger, T. J. J. Müller, *J. Org. Chem.* **2017**, *82*, 567 – 578.

[14] S. Miao, C. G. Bangcuyo, M. D. Smith, U. H. F. Bunz, *Angew. Chem. Int. Ed.* **2006**, *45*, 661 – 665; *Angew. Chem.* **2006**, *118*, 677 – 681.

[15] a) F. K. Merkt, S. P. Höwedes, C. F. Gers-Panther, I. Gruber, C. Janiak, T. J. J. Müller, *Chem. Eur. J.* **2018**, *24*, 8114 – 8125; b) F. K. Merkt, T. J. J. Müller, *Sci. China Chem.* **2018**, *61*, 909 – 924.

[16] H. T. Black, I. Pelse, R. M. W. Wolfe, J. R. Reynolds, *Chem. Commun.* **2016**, *52*, 12877 – 12880.

[17] C. Pathirana, P. R. Jensen, R. Dwight, W. Fenical, *J. Org. Chem.* **1992**, *57*, 740 – 742.

[18] For recent articles see: a) R. Pashazadeh, P. Pander, A. Lazauskas, F. B. Dias, J. V. Grazulevicius, *J. Phys. Chem. Lett.* **2018**, *9*, 1172 – 1177; b) A. A. Kalinin, S. M. Sharipova, T. I. Burganov, A. I. Levitskaya, Y. B. Dudkina, A. R. Khamatgalimov, S. A. Katsyuba, Y. H. Budnikova, M. Yu. Balakina, *Dyes Pigm.* **2018**, *156*, 175 – 184.

[19] S. P S Hirame, R. B. Bhosale, in *Green Chemistry* (Eds.: H. E.-D. M. Saleh, M. Koller), IntechOpen Ltd, London, UK, **2018**, Chapter 9 *Green Approach in Click Chemistry*, pp 171 – 180, DOI: https://doi.org/10.5772/intechopen.72928.

[20] C. Menendez, S. Gau, S. Ladeira, C. Lherbet, M. Baltas, *Eur. J. Org. Chem.* **2012**, 409 – 416.

[21] A. Keivanloo, M. Bakherad, F. Abbasi, T. Besharati-Seidani, A. H. Amin, *RSC Adv.* **2016**, *6*, 105433 – 105441.

[22] For recent reviews, see: a) T. J. J. Müller, *Drug Discovery Today Technol.* **2018**, *29*, 19 – 26; b) F. K. Merkt, T. J. J. Müller, *Isr. J. Chem.* **2018**, *58*, 889 – 900; c) L. Levi, T. J. J. Müller, *Eur. J. Org. Chem.* **2016**, *2016*, 2902 – 2918; d) L. Levi, T. J. J. Müller, *Chem. Soc. Rev.* **2016**, *45*, 2825 – 2846.

[23] N. Nirmalananthan, T. Behnke, K. Hoffmann, D. Kage, C. F. Gers-Panther, W. Frank, T. J. J. Müller, U. Resch-Genger, *J. Phys. Chem. C* **2018**, *122*, 11119 – 11127.

[24] E. Merkul, J. Dohe, C. Gers, F. Rominger, T. J. J. Müller, *Angew. Chem. Int. Ed.* **2011**, *50*, 2966 – 2969; *Angew. Chem.* **2011**, *123*, 3023 – 3026.

[25] C. Boersch, E. Merkul, T. J. J. Müller, *Angew. Chem. Int. Ed.* **2011**, *50*, 10448 – 10452; *Angew. Chem.* **2011**, *123*, 10632 – 10636.

[26] a) C. Janiak, *J. Chem. Soc. Dalton Trans.* **2000**, 3885 – 3896; b) X.-J. Yang, F. Drepper, B. Wu, W.-H. Sun, W. Haehnel, C. Janiak, *Dalton Trans.* **2005**, 256 – 267 and Supplementary Material therein.

[27] S. Fery-Forgues, D. Lavabre, *J. Chem. Educ.* **1999**, *76*, 1260 – 1264.

[28] N. Boens, W. Qin, N. Basarić, J. Hofkens, M. Amelot, J. Pouget, J.-P. Lefèvre, B. Valeur, E. Gratton, M. van de Ven, N. D. Silva Jr., Y. Engelborghs, K. Willaert, A. Sillen, G. Rumbles, D. Phillips, A. J. W. G. Visser, A. van Houk, J. R. Lakowicz, H. Malak, I. Gryczynski, A. G. Szabo, D. T. Krajcarski, N. Tamai, A. Miura, *Anal. Chem.* **2007**, *79*, 2137 – 2149.

[29] M. J. Frisch, G. W. Trucks, H. B. Schlegel, G. E. Scuseria, M. A. Robb, J. R. Cheeseman, G. Scalmani, V. Barone, B. Mennucci, G. A. Petersson, H. Nakatsuji, M. Caricato, X. Li, H. P. Hratchian, A. F. Izmaylov, J. Bloino, G. Zheng, J. L. Sonnenberg, M. Hada, M. Ehara, K. Toyota, R. Fukuda, J. Hasegawa, M. Ishida, T. Nakajima, Y. Honda, O. Kitao, H. Nakai, T. Vreven, J. A. Montgomery, Jr., J. E. Peralta, F. Ogliaro, M. Bearpark, J. J. Heyd, E. Brothers, K. N. Kudin, V. N. Staroverov, R. Kobayashi, J. Normand, K. Raghavachari, A. Rendell, J. C. Burant, S. S. Iyengar, J. Tomasi, M. Cossi, N. Rega, J. M. Millam, M. Klene, J. E. Knox, J. B. Cross, V. Bakken, C. Adamo, J. Jaramillo, R. Gomperts, R. E. Stratmann, O. Yazyev, A. J. Austin, R. Cammi, C. Pomelli, J. W. Ochterski, R. L. Martin, K. Morokuma, V. G. Zakrzewski, G. A. Voth, P. Salvador, J. J. Dannenberg, S. Dapprich, A. D. Daniels, O. Farkas, J. B. Foresman, J. V. Ortiz, J. Cioslowski, D. J. Fox, GAUSSIAN 09 (Revision A.02) Gaussian, Inc., Wallingford CT, **2009**.

[30] a) C. Lee, W. Yang, R. G. Parr, *Phys. Rev. B* **1988**, *37*, 785 – 789; b) A. D. Becke, *J. Chem. Phys.* **1993**, *98*, 1372 – 1377; c) A. D. Becke, *J. Chem. Phys.* **1993**, *98*, 5648 – 5652; d) K. Kim, K. D. Jordan, *J. Phys. Chem.* **1994**, *98*, 10089 – 10094; e) P. J. Stephens, F. J. Devlin, C. F. Chabalowski, M. J. Frisch, *J. Phys. Chem.* **1994**, *98*, 11623 – 11627.

[31] R. Krishnan, J. S. Binkley, R. Seeger, J. A. Pople, *J. Chem. Phys.* **1980**, *72*, 650 – 654.

[32] G. Scalmani, M. J. Frisch, *J. Chem. Phys.* **2010**, *132*, 114110.

Manuscript received: January 18, 2019
Accepted manuscript online: February 11, 2019
Version of record online: April 9, 2019